Appl. Phys. B 71, 593–600 (2000) / Digital Object Identifier (DOI) 10.1007/s003400000265

Applied Physics B
Lasers
and Optics

Dependence of the lidar signal depolarization on the receiver's field of view in the sounding of fog and clouds

B. Tatarov, T. Trifonov, B. Kaprielov, I. Kolev

Institute of Electronics, Bulgarian Academy of Sciences, 72 Tsarigradsko shosse blvd. Sofia 1784, Bulgaria
(Fax: +359-2/975-3201, E-mail: blteam@ie.bas.bg)

Received: 6 September 1999/Revised version: 7 February 2000/Published online: 6 September 2000 –

Abstract. We report an experimental study of the lidar signal depolarization as a function of the relative contribution of the multiple scattering in case of optically dense objects in the atmospheric planetary boundary layer. Results of the observation of fog and stratus clouds are presented, as well as those obtained by sounding of stratocumulus clouds during a snowfall. The lidar data point to a rise of the depolarization coefficient as the influence of the multiple scattering increases in consequence of both viewing angle enlargement and penetration into the object sounded. The variations of the depolarization coefficient are studied as a function of the field of view. In the case of fog, this dependence is approximated by a three-parameter exponential law; it is found that the depolarization increases steeply when the viewing angle is increased from 9 mrad to 12.5 mrad. The relationships between the approximation parameters and the microphysical characteristics of the scattering medium are considered. The experimentally determined size of the area where multiple scattering occurs is in good agreement with that calculated according to the diffusion model. The results obtained on the multiple scattering effect on the depolarization can also be employed in determining the extinction coefficient profiles in optically dense objects, as well as in evaluating the characteristic size of the scattering particles.

PACS: 42.68.Wt; 42.68.Ge; 42.68.Mj

Optically dense atmospheric objects are of considerable interest and are being investigated for the needs of the atmospheric optics as well as the meteorology and geophysics. The lidar techniques for atmospheric studies are among the most powerful means not only for determining the characteristics of atmospheric formations, but also for investigating the processes of their formation and development.

The classical lidar equation determines the power of the received radiation in terms of two unknown quantities: the backscattering and extinction coefficients as functions of the range. If the scattering object is of high optical density, the lidar return is strongly affected by multiple scattering. To describe properly the lidar signal under such conditions, one needs to know one more characteristic, namely, the scattering phase function as a function of the range.

The scattering process leads to changes not only in the signal's power, but also in its state of polarization. A detailed description of the process of light scattering by small particles is given by van de Hulst [1]. According to it, the polarization state of the scattered radiation does not change in the cases of forward- and backscatterings from spherical particles. When one deals with multiple scattering, however, the lidar return is depolarized, even if scattering from spherical particles takes place [2–6]. This opens up the possibility, considered in a number of publications, to detect multiple scattering and to estimate its relative contribution to the lidar signal by determining its polarization characteristics. This approach, however, is only applicable to the case of strictly spherical particles, which is fulfilled to a satisfactory degree for a number of optically dense atmospheric objects, such as water-droplet clouds and fogs. In contrast, for quite a few atmospheric formations, the approximation for particle sphericity does not hold. For this reason, a considerable number of experiments on determining the multiple scattering contribution have been directed to measuring the lidar signal at different viewing angles of the receiver, with a view to obtaining independently the signals arising from single and multiple scatterings [4, 7]. In several papers the use of lidars was reported, since this allows for simultaneous signal registration at different viewing angles by means of coaxial detectors [8], as well as ones for sequential signal recording at different fields of view [3, 4].

A solution to the problem of lidar signal determination in the presence of multiple scattering has also been sought in a number of theoretical papers [7, 9–12]. Various models were proposed to describe the scattering processes, both in cases of double and real multiple scattering. In order to develop adequate and reliable models describing the processes involved in the lidar remote sounding, the results obtained

were compared with data acquired during lidar experiments performed in various atmospheric situations.

This paper presents results of experimental determination of the dependence of the lidar signal polarization characteristics on the receiving viewing angle (field of view, FOV) in the case of sounding optically dense atmospheric objects of the water-droplet type, namely, radiation fog (i.e. fog formed due to night cooling of the air below the dew point) and stratus (St) clouds [13]. Experimental data obtained in the case of sounding stratocumulus (Sc) cloud formations [13] during a snowfall are also considered. These are among the most widely encountered natural optically dense objects in the low atmosphere which is the reason why we felt that these investigations would be of considerable scientific and practical interest.

1 Lidar equipment and experimental

The experiments were carried out using a polarization lidar with a variable receiving FOV. The design of the system was based on an already operating polarization lidar [14]; Table 1 summarizes the main parameters of the lidar system.

The spatial resolution of the lidar system was determined by the ADC clock frequency (20 MHz) and was $\Delta r = 7.5$ m. The corresponding temporal resolution was $\Delta t = 50$ ns, while the time interval between two laser shots was $\Delta t_{\mathrm{rep}} = 0.08$ s (repetition rate of 12.5 Hz).

The experimental data were acquired consecutively by changing the FOV and recording simultaneously the two polarization components of the lidar signal, namely, parallel (P_{p}) and perpendicular (P_{c}) that of to the sounding radiation. The signals were averaged for 32 laser shots and normalized with respect to the power of the sounding laser pulse.

Since the lidar power received diminishes with the square of the range [15], the signals were corrected accordingly. This improved to a considerable degree the visualization and interpretation of the lidar returns.

The depolarization coefficient profile ($\delta(r)$) along the sounding path was obtained by calculating its values for each point along the path as the ratio:

$$\delta(r) = \frac{\overline{P}_{\mathrm{c}}(r)}{\overline{P}_{\mathrm{p}}(r)}, \qquad (1)$$

where $\overline{P}_{\mathrm{p}}$ and $\overline{P}_{\mathrm{c}}$ are the averaged values of P_{p} and P_{c}, respectively.

2 Experimental conditions and objects sounded

During the experiments described here, the lidar was placed in a south-eastern part of the city of Sofia (42°3′ N, 23°23′ E, 591 m above MSL), near the Institute of Electronics.

A characteristic feature of the sounding path is the existence of two zones. The first one is an open grass area taking up approximately the first 300 m of the horizontal distance. A residential district follows which covers the distance from 300 m to 1000 m along the path. The different characteristics of the two zones are responsible for the difference in the processes of heating of the underlying surface, and, subsequently, in the temperature and motion of the air masses [16]. These particularities influence considerably the lidar returns in the presence of fog in the region of the experiment, but play a negligible role when cloud formations are sounded.

The scattering properties of the objects sounded are determined by the chemical content, the size, the shape, and the concentration of the particles, as well as by the wavelength of sounding radiation. Radiation fog and St and Sc clouds have similar chemical content, namely, water droplets with index of refraction $n = 1.33$. Variations in their chemical composition could arise from their being formed by different mechanisms in different areas. Since the goal of the present paper is to determine the dependence of the lidar signal depolarization on the receiving FOV, the existence in the constituting particles of additives with a chemical composition different from that of water will be neglected.

The shape of the particles present in all three atmospheric formations is close to spherical; consequently, single scattering at angles of 0° and 180° takes place without change in the polarization state. To a high degree of accuracy, water-droplet clouds and fogs can be considered as polydisperse systems in what concerns the size of the constituting particles [13, 17]; i.e., as ensembles of particles with the same size and optical constants, and differing only in their size. To describe the scattering properties of, such a system, one can make use of the so-called particle size distribution function ($f(\varrho)$) which describes the particles' concentration in terms of the particles radii (ϱ). In all three types of objects studied, the density of the particles size distribution could be assumed to be of a modified gamma-type [17]. Its precise form is determined

Table 1. Main parameters of the lidar system

Laser source		Receiver		Data acquisition and processing set	
Gain medium	Nd:YAG, Q-switched	Telescope	Cassegrainian	Analog-to-Digital Converter	2× HP5180A 10 bit, 20 MHz
		Main mirror diameter	150 mm		
Polarization	linear	Equivalent focal length	2250 mm		
Operational wavelength	532 nm	Fields of view	1.5–15 mrad, step of 0.5 mrad	Computer	standard PC
Pulse energy	15 mJ				
Pulse width	15 ns	Detection	2 polarizations		
Repetition rate	12.5 Hz	Detectors	2× photomultipliers FEU-84		
Diameter of the laser beam	1 cm	Interference filter FWHM	1 nm		
Divergence	1.5 mrad				

by the modal radius of the particles and by two constants defining the distribution density. The particles' modal radius is the one where the particles' size distribution function has an absolute maximum. The values of the modal radius and the two constants are different for the different objects sounded, and, correspondingly, the respective size distributions are also different. Another characteristic of the particles used throughout the paper is their effective diameter d_{eff} [10]:

$$\frac{d_{\text{eff}}}{2} = \frac{\langle \varrho^3 \rangle}{\langle \varrho^2 \rangle} = \frac{\int_0^\infty \varrho^3 f(\varrho) \mathrm{d}\varrho}{\int_0^\infty \varrho^2 f(\varrho) \mathrm{d}\varrho} . \quad (2)$$

The particles' sizes for all three types of formations fall within the range from one to several tens of microns; the most common distributions are characterized by modal radii from 3–4 μm for radiation fog, 5–6 μm for St clouds and 8–9 μm for Sc clouds; these values are taken from model descriptions of the objects for the respective season and geographical location. The particles' sizes are several times bigger than the wavelength of the sounding radiation. Under such conditions – photons scattered by particles considerably larger than the wavelength – the larger part of the scattered energy is concentrated in the forward diffraction peak [7].

3 Lidar polarization measurements in the case of radiation fog

The data were acquired on 6 December 1996, in still conditions at a meteorological visibility $S_{\text{m}} \approx 1$ km and air temperature 3 °C. The lidar system was located within the zone covered by fog. The sounding was performed along a slant path at an angle of 21°. According to an independent lidar observation, the fog was uniform in the horizontal direction and the extinction coefficient was determined to be $\alpha_{\text{ext}} \approx 4\,\text{km}^{-1}$.

3.1 Lidar signals in the cases of maximum and minimum fields of view

Figure 1 presents typical results of sounding in fog at maximum field of view (15 mrad, FOV $= 10\theta_{\text{laser}}$), i.e., when a component arising from multiple scattering is present in the lidar response.

Two regions along the sounding path can clearly be distinguished characterized by different behavior of the polarized components and the depolarization profiles. The first one spans the distance from the lidar location to approximately 350 m along the path, the second one lies between 350 m and 500 m. These regions obviously correspond to the two specific types of underlying surface as described above.

The lidar signal profiles exhibit a small increase within the 100–350 m zone; this is due to an increase in the particles concentration in the vertical direction. This most probably results from the fact that during the convective boundary layer development the processes of fog dissipation take place in the vertical direction in the presence of a temperature inversion at an altitude of more than 200 m. The depolarization in this zone grows from about 3% at the beginning to about 9% at a distance of 350 m along the sounding path – a rate of 3%/100 m ($\approx 0.3\%\,\text{km}^{-1}$). This increase is due to a rise in the relative contribution of the multiple scattering to the lidar response as the distance of sounding within the fog is increased.

A substantial difference in the behavior of the lidar responses is seen at distances along the sounding path exceeding 350 m, corresponding to an altitude of approximately 125 m. Within an interval of about 100 m (distance from 360 m to 460 m) the lidar response amplitude drops by a factor of almost ten. The near constant slope of the lidar profiles indicate that the atmosphere in that region is homogeneous. This fact suggests that the decrease in the lidar returns amplitude is due to attenuation in a zone with high optical density which implies an increased role of the multiple scattering in that zone. The increase of the relative contribution of the multiple scattering is substantiated by the behavior of the depolarization ratio in this part of the sounding path: the depolar-

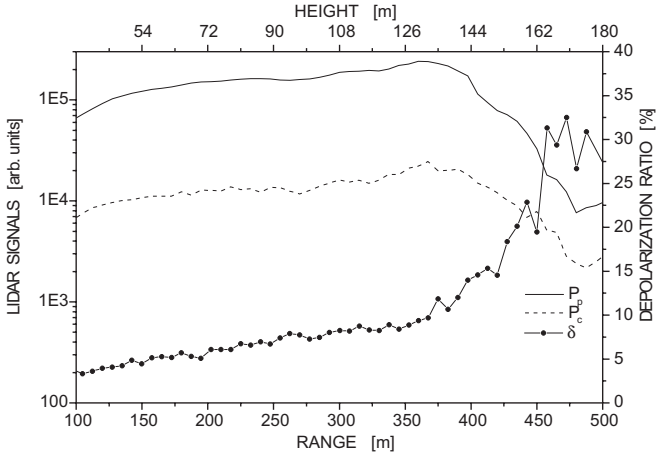

Fig. 1. Lidar signals and depolarization (δ) profiles in the case of radiation fog at a field of view of 15 mrad (FOV $= 10\,\theta_{\text{laser}}$); 12:37 LST, December 6, 1996; P_{p} and $P_{\text{c}-}$. lidar signals with polarization parallel and perpendicular with respect to that of the sounding radiation

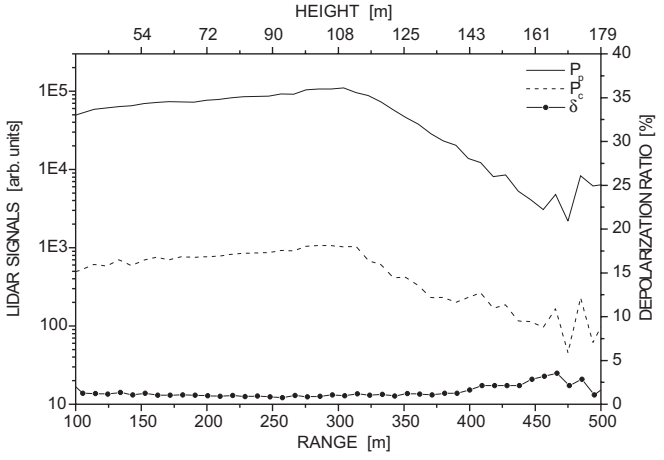

Fig. 2. Lidar signals and depolarization (δ) profiles in the case of radiation fog at a field of view of 1.5 mrad (FOV $= \theta_{\text{laser}}$); 12:39 LST, December 6, 1996; P_{p} and $P_{\text{c}-}$. lidar signals with polarization parallel and perpendicular with respect to that of the sounding radiation

ization increases from a value of approximately 9% to about 30%, i.e. by a factor of three within 100 m ($\approx 200\%\,\mathrm{km}^{-1}$).

Figure 2 shows the profiles of the lidar signal polarized components and the depolarization ratio at a field of view of 1.5 mrad (FOV $= \theta_{\mathrm{laser}}$) taken immediately after (12:39 LST) those shown in Fig. 1. Receiving signals at such FOV should eliminate the effect of the off-axis multiple scattering.

As it is seen, the decrease of the FOV results in a decrease of the amplitudes of both lidar return components; however, the extent of this decrease is different: the drop in the parallel component is 10%–20%, whereas the perpendicular diminishes by a factor of almost 10. As a consequence, the depolarization ratio also decreases.

The zone of the weak increase of the signal is smaller and occupies the distance up to 300 m along the sounding path. When the influence of the multiple scattering is eliminated, the part of the sounding path of high optical density begins at about 300 m and reaches up to 475 m. The change in the boundary distances of the zones considered (Figs. 1 and 2) is associated with the loss of the signal local belonging. The latter is a result of the presence of multiple scattering. The extinction coefficient in the zone 300–475 m was determined to be $\alpha_{\mathrm{ext}} = 11\,\mathrm{km}^{-1}$, as calculated using the slope method $\left(\alpha_{\mathrm{ext}} = -\frac{0.5}{r_2 - r_1} \ln\left(\frac{P(r_2)}{P(r_1)}\right)\right)$.

One can see that at a FOV close to the laser beam divergence the depolarization coefficient assumes values of $\approx 1\%$–2%, corresponding to single scattering (Fig. 2). At distances of up to 400 m along the sounding path, the depolarization curve is flat, i.e., the increase seen in Fig. 1 is not present. In the 400–475 m range, the depolarization grows by 1%–2%. The fact that the value of the depolarization ratio decreases in the sounding range up to 300 m when the FOV is narrowed is an unambiguous indication for the presence of multiple scattering in the case of the large viewing angle.

3.2 Depolarization of the lidar signal at different fields of view of the receiver

The lidar data discussed so far were obtained during sounding of a radiation fog and exhibited substantial differences in their polarization parameters in the cases of maximum and minimum FOV. To obtain information about the polarization characteristics when the multiple scattering influence varies, we studied the behavior of the depolarization ratio as a function of the FOV of the receiver.

3.2.1 Experiment. The experiment consisted of a consecutive recording of the polarized components of the lidar signal at different receiving FOV within the 1.5–15 mrad (FOV $= \theta_{\mathrm{laser}} - 10\theta_{\mathrm{laser}}$) interval at a step of 0.5 mrad. Based on the lidar profiles obtained, the depolarization ratio corresponding to the respective viewing angle was calculated. Figure 3 shows the depolarization ratio variation as a function of the field of view ($\delta = \delta(\mathrm{FOV})$) at a sounding distance of 360 m.

It is seen that at viewing angles close to the laser beam divergence, the depolarization coefficient is about 1%–2%. This value remains constant when the FOV is increased from 1.5 mrad to about 9 mrad. The depolarization ratio rises steeply when the viewing angle is increased from 9 mrad to 12.5 mrad. Increasing FOV over 12.5 mrad practically does not change the depolarization ratio value (about 11%). Since

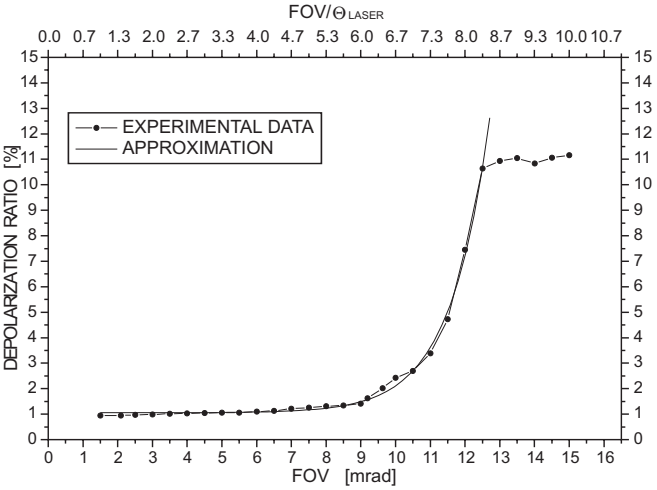

Fig. 3. Depolarization ratio dependence on the receiving field of view in the case of radiation fog

the only parameter varied during the experiment is the lidar FOV, the depolarization changes can be considered as due to the different contribution of the multiple scattering.

The presence of the multiple scattering suggests more than one scattering event. In the case of the particular lidar configuration and geometry of sounding, it can be assumed with a reasonable accuracy that the multiple scattering contribution to the lidar return is mainly made up of double scattering or multiple small-angle forward scatterings and one backscattering at an angle close to 180°.

A diagram of the double scattering process is shown in Fig. 4. The optically dense object there is located at a distance r_0 (in the case considered $r_0 = 0$). The first scattering of the sounding radiation at angle φ_1 occurs from a particle at a distance r_{F}. The already scattered light undergoes a second scattering event at an angle φ_2 at a distance r_{S} and is then collected by the receiving antenna. The depolarization coefficient of the radiation thus received is determined by its dependence on the scattering angles $\delta = \delta(\varphi)$.

According to that scheme the results shown in Fig. 3 could be discussed as follows.

At angles close to the laser beam divergence, the depolarization coefficient values of about 1%–2% correspond to scattering from spherical particles in the single-scattering approximation [1]. Due to the small viewing angles, backscattering within FOVs close to the laser beam divergence proceeding at angles close to 180° does not cause depolarization of the received radiation.

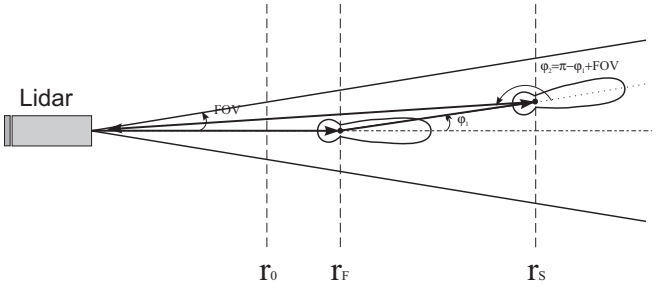

Fig. 4. Schematic diagram of the process of double scattering

With the increase of the FOV, multiply scattered radiation begins to be collected. The maximum value of the first scattering angle (φ_1, Fig. 4) is determined by the viewing angle of the lidar, the distance to the object, and the penetration depth. The depolarization coefficient of the radiation received is determined by its dependence on the scattering angle $\delta = \delta(\varphi)$. In its turn, this dependence is determined by the scattering phase function $ph(\varphi)$. For the object discussed (radiation fog), having effective particle diameter $d_{\text{eff}} \approx 2\,\mu\text{m}$, the phase function is characterized by a maximum in the forward direction (due to diffraction) with a nearly Gaussian shape and a width determined by the ratio $\lambda/\pi d$.

The $\delta(\varphi)$ dependence can be calculated using the models presented in [17]. For the specific conditions of our experiment, the $\delta(\varphi)$ dependence takes values close to zero not only for scattering angle $\varphi = 0°$, but also for angles differing from zero by a few degrees. By the same token, it also assumes a value of zero at scattering angle $\varphi = 180°$. But, in contrast to the forward scattering ($\varphi = 0°$), it grows considerably at angles differing from 180° by a few mrad. Thus, at small viewing angles (but still larger than the lidar beam divergence), the lidar receives multiply (doubly) scattered radiation, for which $\varphi_1 \approx 0°$, and $\varphi_2 \approx 180°$, and, therefore, depolarization is not observed. As the FOV grows, the lidar collects not only light scattered by the mechanism just described, but also multiply scattered light formed by scattering events for which φ_1 differs significantly from 0°, and φ_2, from 180°. The depolarization of the radiation received remains close to its values for single scattering so long as φ_1 and φ_2 take values such that $\delta(\varphi) = 0$. For the experimentally measured depolarization dependence shown in Fig. 3, this holds true up to FOV = 9 mrad. In the range from 9 mrad to 12.5 mrad, δ(FOV) grows due to the fact that the receiving system collect light for which φ_2 is such that $\delta(\varphi_2) \neq 0$.

The above discussion leads one to the conclusion that the steep increase of δ(FOV) in the 9–12.5 mrad range is a result of the behavior of $\delta(\varphi)$ (or, respectively, of $ph(\varphi)$. A confirmation of this proposition is given by the numerical simulation concerning the size of the region where multiple scattering takes place. The results of that simulation are presented in Fig. 5. As one can see, for the distance considered ($r = 360$ m), multiple scattering is also present in the region below 9 mrad, but takes place at such angles that the light is not depolarized significantly.

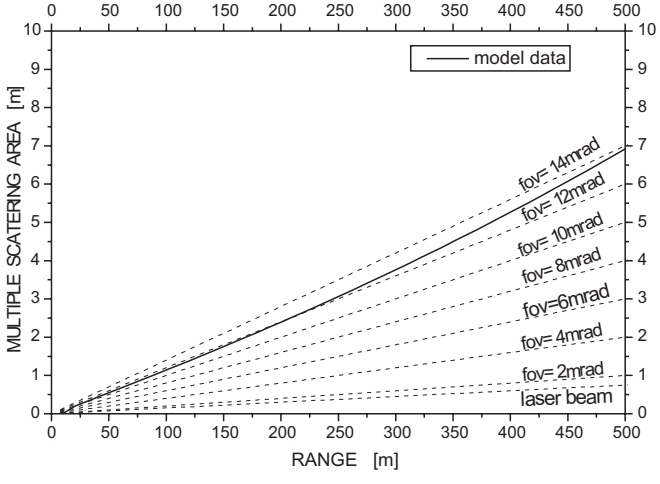

Fig. 5. Dependence of the diameter of the spatial region giving rise to multiply scattered signal on the distance along the sounding path

Based on the assumption of spherical scattering centers, and bearing in mind the dependence shown in Fig. 3, one could draw the conclusion that for the case discussed (radiation fog), the effects of multiple scattering are detectable within a volume determined by a field of view of 12.5 mrad (FOV $= 8.7\theta_{\text{laser}}$). An increase of the FOV above 12.5 mrad does not result in an increase of the multiply scattered signal. Thus, the dependence discussed allows one to determine the size of the area where multiple scattering occurs. The fact that the constant value of the depolarization ($\approx 11\%$) when the FOV rises above 12.5 mrad is due to the dimension of the volume where multiple scattering takes place, rather than to the phase function behavior, is confirmed by the discussion in Sect. 3.2.3.

3.2.2 Approximation of the experimental data. The depolarization ratio dependence on the receiving FOV in the 1.5–12.5 mrad range was found to have an exponential shape that can be approximated with high accuracy by the expression

$$\delta = a + b\exp(c\,\text{FOV})\,, \tag{3}$$

where $a = 1.05$, $b = 1.6 \times 10^{-4}$, $c = 0.88$.

The calculations were made using depolarization ratio and FOV dimensions (%) and (mrad), respectively. The fit was performed employing the least-squares method by minimizing the value of χ^2. In our case the value of the deviation turned out to be $\chi^2 = 0.018$. The fitting curve drawn with the above parameters is shown in Fig. 3 by a solid line.

The coefficients in relation (3) can be considered as parameters depending on the microphysical characteristics of the scattering centers (shape, size distribution function, etc.) and on the optical density of the medium. According to Samohvalov's theoretical model [11], in the approximation of double scattering in a homogeneous medium, the depolarization coefficient is uniquely defined if the distance to the object sounded, the lidar's field of view, and the medium's scattering matrix are known. Since in the experiment reported here the distance to the object and the field of view are known (measurable), the depolarization ratio value is determined by the scattering matrix components. Thus the three coefficients in the approximation derived (3) are functions of the scattering matrix components, and, respectively, of the microphysical properties of the scattering centers. Furthermore, the scattering matrix components determine also the phase function $ph(\varphi)$ and the $\delta(\varphi)$ dependence.

Relation (3) is a sum of two components, namely, a and $b\exp(c\,\text{FOV})$. The first one, the parameter a, has a contribution to the depolarization ratio value that does not depend on the receiving FOV. This enables one to relate it to that part of backscattered radiation depolarization which is due to the nonsphericity of the scattering particles. In fact, according to (3), at fields of view approximately equal to the laser beam divergence, when the multiple scattering contribution is eliminated, the addend $b\exp(c\,\text{FOV}) \approx 0$, and the depolarization of the lidar signal received is approximately equal to a ($\delta \approx a$).

The other two parameters are multiplicands in the second term of the expression. One can see that the parameter c determines the rate of depolarization increase with the FOV, while b establishes the minimum FOV where the depolarization becomes detectable. The exact relationships between the parameters b and c and the scattering phase function $ph(\varphi)$ are under study and this is the aim of a future report.

Similar relations (with small differences in the values of a, b, and c) were constructed for the distances from 260 m to 460 m along the sounding path. The main difference observed in the curves' behavior at different distances is in the value of the depolarization ratio saturation when the FOV is increased above 12.5 mrad, for example, at 460 m it is 30%.

3.2.3 Comparison of the experimental data with a theoretical model. The results presented in the previous section concerning the size of the area where multiple scattering occurs agree well with the values calculated according to the diffusion model following the technique proposed by Bissonnette [10]. In Fig. 5 the solid line presents the diameter (D) of the region from where the multiply scattered radiation originates before being received by the telescope as a function of the distance along the sounding path.

The formula used to determine the diameter D is as follows [10]:

$$D^2 = z'^2\theta_{\text{laser}} + \frac{2\gamma}{A_1}\int_{z'}^{z} \frac{\exp[\frac{1}{2}\tau(z'') - \tau(z')] - 1}{y(z'')[\tau(z'') - \tau(z')]}(z'' - z')\mathrm{d}z'' , \tag{4}$$

where θ_{laser} is the laser beam divergence, z is the distance along the sounding path, z' is the distance to the object sounded, $\tau(z) = \int_0^z \alpha_{\text{ext}}(z')\mathrm{d}z'$ is the optical density of the medium, $y(z) = \pi d_{\text{eff}}/\lambda$ is a dimension parameter, d_{eff} is the effective diameter of the scattering centers, λ is the operating wavelength, z'' is a current variable, and γ and A_1 are constants.

The calculations were performed by means of an adaptive numerical integration procedure based on the Simpson formula [18]. The following values of the parameters were used: extinction coefficient $\alpha_{\text{ext}} = 4\,\text{km}^{-1}$, effective particle diameter $d_{\text{eff}} = 2\,\mu\text{m}$, laser beam divergence $\theta_{\text{laser}} = 1.5$ mrad, and Gaussian shape of the phase function peak. The laser beam diameter and the FOV diameter at different viewing angles are also denoted in Fig. 5.

It is clearly seen that the diameter of the region where multiple scattering takes place is approximately equal to that determined by a FOV of 13 mrad. The experimentally determined viewing angle beyond which one does not observe an increase of the multiple scattering is 12.5 mrad. This is in good agreement with the diffusion model data at parameters values as defined above.

4 Depolarization measurements in the case of cloud formations

This section summarizes experimental results obtained in the case of sounding of clouds. Different types of clouds were studied, namely, of water-droplet type and with mixed phase composition.

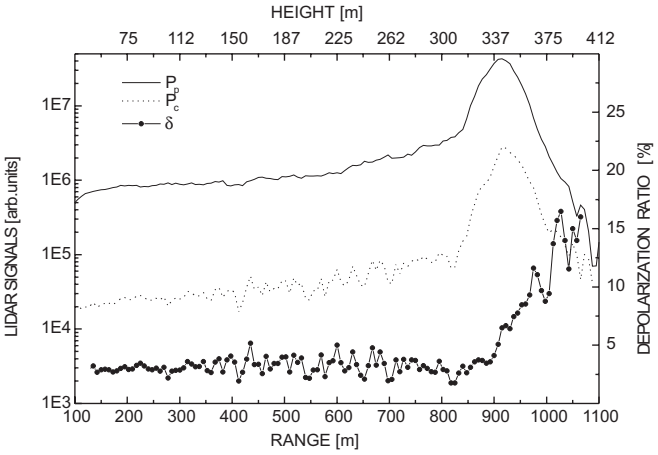

Fig. 6. Lidar signals and depolarization (δ) profiles in the case of St clouds at a field of view 15 mrad (FOV $= 10\theta_{\text{laser}}$), 13:30 LST on January 7, 1997; P_{p} and $P_{\text{c}-}$. lidar signals with polarization parallel and perpendicular with respect to that of the sounding radiation

4.1 Sounding of stratus clouds

The lidar experiment was carried out on January 7, 1997, under the following meteorological conditions: air temperature 0–2 °C, wind velocity $\approx 10\,\text{ms}^{-1}$, meteorological visibility at the earth's surface $S_{\text{m}} \approx 10$ km, altitude of cloud base 300–400 m. The sounding was performed at an angle of 22°.

Figure 6 shows the lidar profiles obtained at a FOV of 15 mrad (FOV $= 10\theta_{\text{laser}}$) at 13:30 LST.

The curves of the two polarized components show a rise in the lidar response with the laser beam penetration into the cloud volume. The distance to the cloud base along the sounding path (according to the first-derivative method [19]) is about 830 m, corresponding to an altitude of 320 m. The lidar signal reaches a maximum at about 920 m, and decreases afterwards due to the strong extinction of the laser by radiation within the cloud. One should note that the cross-polarized component maximum is delayed by about 100–150 ns with respect to that of the parallel component. The depolarization ratio profile is flat between the ground and the cloud base; its values of 2%–3% correspond to scattering from near-spherical particles.

In the range of few tens of meters around the cloud base, the depolarization decreases to about 2%. As the laser beam penetrates further into the cloud, the depolarization ratio increases up to approximately 15%. The depolarization ratio behavior within the cloud volume can be divided into two zones: the first one near the cloud bottom, and the second beyond the signal maximum. The difference between the two zones is in the rate of depolarization ratio growth: in the former, the growth is from 2% to 5% for about 100 m ($\approx 30\%\,\text{km}^{-1}$), whereas within the latter it is from 5% to 15% for the same distance ($\approx 100\%\,\text{km}^{-1}$).

Figure 7 presents lidar data obtained by sounding the same cloud as above, but at a FOV 1.5 mrad, i.e., equal to the laser beam divergence. The measurement took place at 13:31 LST.

The lidar returns from the cloud received at the minimum FOV are of smaller amplitude for both polarized components as compared to those at the maximum FOV. The peak of the cross-polarized component is not shifted with respect to the

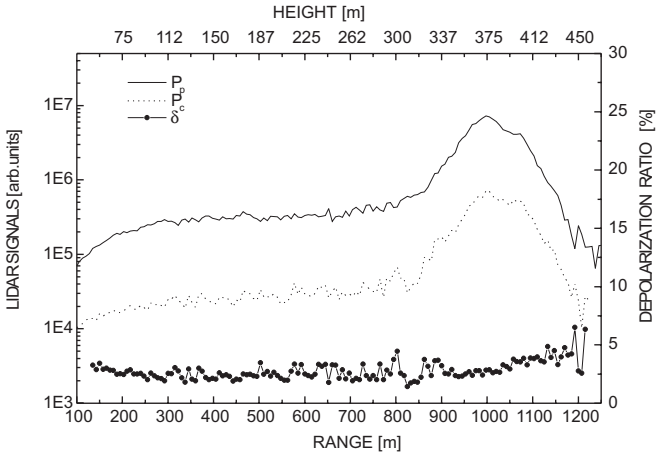

Fig. 7. Lidar signals and depolarization (δ) profiles in the case of St clouds at a field of view 1.5 mrad (FOV $= \theta_{\text{laser}}$), 13:31 LST on Jan. 7, 1997; P_{p} and $P_{\text{c}-}$. lidar signals with polarization parallel and perpendicular with respect to that of the sounding radiation

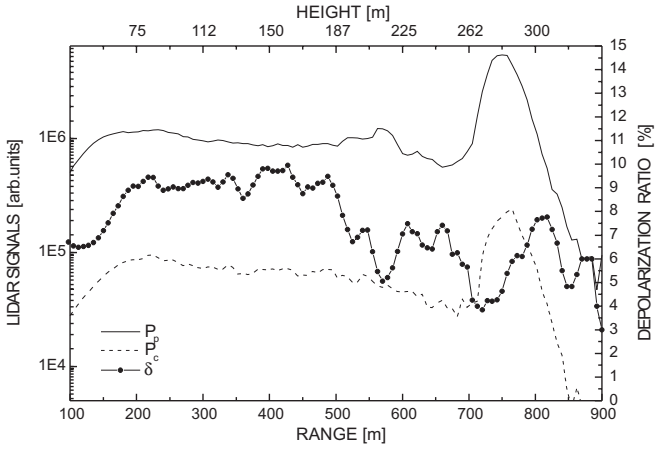

Fig. 8. Lidar signals and depolarization (δ) profiles in the case of Sc clouds during wet snowfall at a field of view of 15 mrad (FOV $= 10\theta_{\text{laser}}$); 17:08 hours local time on Feb. 8, 1997; P_{p} and $P_{\text{c}-}$. lidar signals with polarization parallel and perpendicular with respect to that of the sounding radiation

parallel one (Fig. 7), which proves that the delay observed in Fig. 6 is the result of multiple scattering. The depolarization ratio behavior within the cloud volume also shows a substantial difference from the earlier results: the depolarization ratio growth is considerably lower: within the cloud (about 300 m) it increases from 2% to 5% (10% km^{-1}); moreover, it is hard to make a distinction between zones in terms of the depolarization ratio rate of growth – the rate is approximately constant along the path within the cloud with a value of about 1% per 100 m (10% km^{-1}).

The lack of local maxima and minima both in the profiles of the polarized components and the depolarization ratio is evidence for the homogeneity of the cloud with respect to the phase composition and particles concentration. These conclusions agree well with the theoretical and applied meteorology concepts concerning the structure of St clouds. As one can see in Fig. 7, the depolarization ratio values do not exceed 5% which is an indication for the absence of crystal (ice) phase.

4.2 Sounding of stratocumulus clouds during snowfall

The experimental data were acquired on 8 February 1997 at 17:08 LST. The meteorological situation was: wind velocity 2–3 ms^{-1}, air temperature ≈ 0 °C, wet snowfall, cloud base at 250 m.

The profiles of the signal's polarized components and the depolarization ratio obtained at a FOV of 15 mrad are presented in Fig. 8.

Both polarized components' profiles show the presence of a cloud layer located at a distance of 700–800 m along the sounding path. Its thickness is probably much larger, but cannot be determined due to the total extinction of the laser radiation. The parallel component profile reveals the existence of another layer of 500–600 m at an altitude of 200 m; it is not well expressed in the cross-component profile. This layer is in fact a sub-cloud formation [20] characterized by lower optical density compared with the cloud itself. The cloud type was determined as Sc; the snowfall originated from a higher nimbus cloud (Ns) [13], located outside the lidar range.

In the range between the ground and the cloud layers, the depolarization ratio is in the 9%–10% interval. These relatively high values are due to the strongly non-spherical shape of the snowflakes. These values, however, are lower than the typical ones (20%–30%) measured during a snowfall [21]. The reason for this is that we performed our experiment during a wet snowfall, i.e., precipitation with mixed phase composition. The depolarization ratio drops down to 5% at a distance of 500 m corresponding to the altitude of the sub-cloud layer.

The depolarization ratio increases along the distance between the two parts of the cloud which is indicative of a higher relative content of ice crystals. The penetration into the denser part of the cloud (700 m) leads to a decrease of the depolarization ratio down to ≈ 4%, which is evidence for the mixed phase composition. Further penetration within the cloud volume results in a rise of the depolarization ratio due to the multiple scattering contribution.

Figure 9 shows lidar data obtained in the same meteorological situation but at a FOV 1.5 mrad (FOV $= \theta_{\text{laser}}$). The shapes of the curves of the polarized components do not exhibit significant changes. The discrepancies with the previous

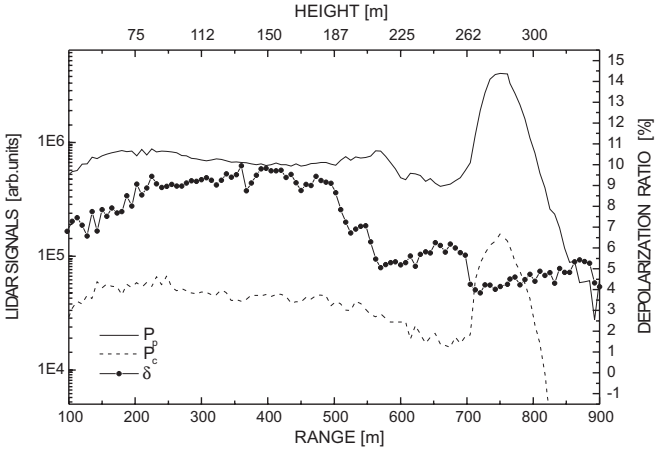

Fig. 9. Lidar signals and depolarization (δ) profiles in the case of Sc clouds during wet snowfall at a field of view of 1.5 mrad (FOV $= \theta_{\text{laser}}$); 17:08 LST on February 8, 1997; P_{p} and $P_{\text{c}-}$. lidar signals with polarization parallel and perpendicular with respect to that of the sounding radiation

case are seen in the depolarization ratio profile. Within the cloud (a 700–800 m range) the depolarization ratio grows at a rate significantly lower than that observed at the maximum FOV. Its value (4%) indicates a low relative content of the crystal (ice) phase. Similar differences can be seen in the depolarization ratio behavior within the sub-cloud formation (≈ 600 m); its higher value there ($\approx 6\%$) is the result of the higher relative content of ice crystals.

As one can see, the depolarization ratio profile does not undergo substantial changes in comparison with the previous observation for distances up to 500 m along the sounding path. The ratio keeps its value of about 9%, even though the multiple scattering contribution has been eliminated, clearly demonstrating that the signal depolarization arises from the existence of ice crystals.

5 Conclusions

The paper presents an experimental study of the relationship between the depolarization of the lidar signal and the multiple scattering contribution. Atmospheric objects of high optical density located within the planetary boundary layer are studied, namely, radiation fog, St clouds and Sc clouds during snowfall. The measurements of the polarization characteristics of the lidar signal reveal a dependence of the depolarization ratio on the type of object sounded, the receiving field of view, and the depth of penetration of the sounding radiation.

At viewing angles close to the laser beam divergence, the depolarization remains approximately constant whereas at angles of about $\mathrm{FOV} = 10\theta_{\mathrm{laser}}$ it increases with the penetration into the object. The different behavior is due to multiple scattering effects; they affect negligibly the lidar signal in the first case ($\mathrm{FOV} = \theta_{\mathrm{laser}}$, whereas in the second ($\mathrm{FOV} = 10\theta_{\mathrm{laser}}$) their contribution is considerable. When the contribution of multiple scattering is eliminated, the depolarization ratio values differ depending on the presence (during snowfall) or absence (in the case of fog or St clouds) of crystal (ice) phase along the sounding path.

Furthermore, the behavior is determined of the lidar signal polarization characteristics for different degrees of the multiple scattering influence in the case of sounding of fog. For this purpose, the depolarization ratio is measured at the different viewing angles of the receiving optics. The experimentally determined dependence of the depolarization on the viewing angles is approximated by a high degree of accuracy by a three-parameter exponential law. The approximation parameters determine: the depolarization in the case of single scattering; the minimum angles at which the depolarization is measurable; and the scattering properties of the medium. These can be used as an independent source of experimental information when lidar signals in the case of multiple scattering are modelled.

Based on the dependence of the depolarization on the receiving viewing angle obtained as described, the area where multiple scattering occurs is determined. The results are in good agreement with numerical simulations based on the diffusion model.

Acknowledgements. The authors wish to thank Prof. L.R. Bissonnette of Defense Research Establishment, Valcartier, Canada for the valuable discussions of the experimental data. The work was supported in part by the National Science Fund at the Ministry of Education, Science, and Technologies of Republic of Bulgaria under Contract F 509.

References

1. H.C. van de Hulst: *Light Scattering by Small Particles* (Wiley, New York 1957)
2. R.J. Allen, C.M.R. Platt: Appl. Opt. **16**, 3193 (1977)
3. M. Kerscher, W. Krichbaumer, M. Noormohammadian, U.G. Oppel: Opt. Rev. **2**, 304 (1995)
4. C. Werner, J. Streicher, H. Herrmann, H.G. Dahn: Opt. Eng. **31**, 1731 (1992)
5. R.H. Dubinsky, A.I. Carswell, S.R. Pal: Appl. Opt. **24**, 1614 (1985)
6. S.R. Pal, A.I. Carswell: Appl. Opt. **12**, 1530 (1973)
7. E. Eloranta: Appl. Opt. **37**, 2464 (1998)
8. D.L. Hutt, L.R. Bissonnette, L. Durand: Appl. Opt. **33**, 2338 (1994)
9. L. Bissonnette, P. Bruscaglioni, A. Ismaelli, G. Zaccanti, A. Cohen, Y. Benayahu, M. Kleiman, S. Egert, C. Flesia, P. Schwendimann, A.V. Starkov, M. Noormohammadian, U.G. Oppel, D.M. Winker, E.P. Zege, I.L. Katsev, I.N. Polonski: Appl. Phys. B **60**, 355 (1995)
10. L. Bissonnette: Appl. Opt. **33**, 6449 (1996)
11. I. Samokhvalov: In *Remote Methods for Investigation of the Atmosphere* (Nauka, Novosibirsk 1980)
12. P. Bruscaglioni, A. Ismaelli, G. Zaccanti: Appl. Phys. B **60**, 325 (1995)
13. World Meteorological Organization, International Meteorological Vocabulary, No. 182, Second edition, (1992)
14. I. Kolev, B. Kaprielov, B. Tatarov: Comptes rendus. de'l Academie bulgare des Sciences **49**, 31 (1995)
15. R.M. Measures: *Laser Remote Sensing Fundamentals and Applications* (Wiley, New York 1984)
16. E. Donev, K. Zeller, S. Panchev, I. Kolev: Acta Meteorologica sinica **9**, 101 (1995)
17. D. Deirmendjian: *Electromagnetic Scattering on Spherical Polydispersions* (Elsevier, New York 1969)
18. M.A. Malcolm, R.B. Simpson: Trans. Math. Software **1**, 129 (1975)
19. S.R. Pal, W. Steinbrecht, A.I. Carswell: Appl. Opt. **31**, 1488 (1975)
20. R.B. Stull: *An Introduction to Boundary Layer Meteorology* (Kluwer, Dordrecht, Boston, London 1988)
21. B. Tatarov, I. Kolev, B. Kaprielov, T. Trifonov: Proc. SPIE **3052**, 294 (1996)